

LabVIEW based HP memristor simulator with hardware connectivity for real time circuit operation

Abhra Majumdar
Electrical Engineering
IIT, Kharagpur
Kolkata, India
abhasky@gmail.com

Abhisek Manna
Applied Electronics & Instrumentation
Engineering
C.V Raman College Of Engineering
Bhubaneswar, India
abhisek77manna@gmail.com

Asutosh Patnaik
Applied Electronics & Instrumentation
Engineering
C.V. Raman College Of Engineering
Bhubaneswar, India
a_patnaik@yahoo.in

Abstract – Memristor has emerged as fourth fundamental element in electronics. However, all the characteristics and functionalities of a memristor are yet to be understood. Main restriction behind wide spread research on this is lack of availability of a physical memristor. This paper presents an easy way to implement memristor simulator using LabVIEW, a powerful virtual instrumentation platform. Here ideal HP memristor model is implemented. Input signal is taken from a physical function generator. It is interfaced with the LabVIEW using an analog to digital converter (ADC) module. Mathematical model of the memristor is implemented virtually in LabVIEW. Output is shown in Digital Storage Oscilloscope (DSO) which is interfaced with LabVIEW using a Digital to Analog converter (DAC) module. Using this setup, a pinched hysteresis loop in Voltage – Current (V – I) characteristics curve which is the signature of a memristor is observed. Shrinkage of loop area with the increment of input frequency is also been observed which concludes success full implementation of the model. Other Input-output parameters are plotted using waveform graph block in software interface. LabVIEW graphical coding is used for all the necessary programmes to implement the model. Although, here ideal HP memristor model is implemented, it can be easily extended to any other memristor models.

Keywords – Memristor, LabVIEW, NI ELVIS, graphical coding, ADC, DAC, simulator, emulator.

I. INTRODUCTION

With the advancement of integrated circuit technology devices are scaled down to nano level, some time in atomic level [1]. But at such small scale while working with unconventional elements, “current-voltage anomalies” are reported in [2][3] which cannot be explained properly with traditional basic elements of electronics i.e. resistor, capacitor and inductor. To address this problem an axiomatic approach was taken by L. Chua[4]. He observed that considering current as the time derivative of the charge and voltage as the time derivative of the flux, a resistor is defined by the relationship between voltage and current as $dv=R*di$, the capacitor is defined by the relationship between charge and voltage as $dq=C*dv$ and the inductor is defined by the relationship between flux and current as $d\phi=Ldi$. Therefore there must be another fundamental circuit element to complete the symmetry of the relation between charge and magnetic flux that is $d\phi=Mdq$. Based on that in the year 1971 he postulated a new device called memristor (short

form of memory resistor) as fourth fundamental component of electronics.

Figure 1 shows the basic relationship among these four fundamental components.

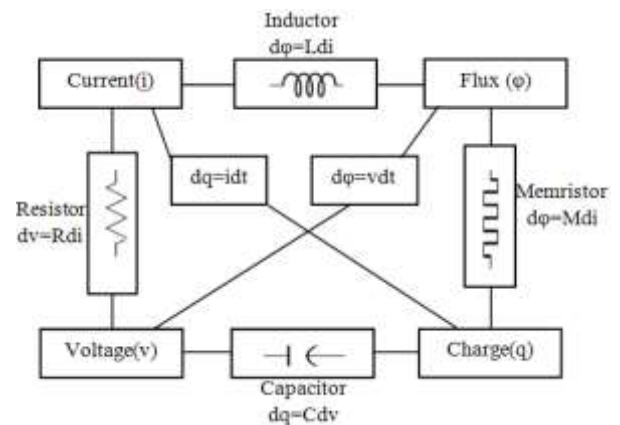


Fig. 1. Four fundamental components of electronics, defined by flux (ϕ), charge (q) and their time derivative voltage (v), current (i).

In already well established theory, relation between voltage and current can be represented by resistance (R) whereas charge-voltage and flux-current relation can be represented by capacitance(C) and inductance (L) respectively. To complete this symmetry there must be a relationship between flux and charge and it is done by memristor (memory resistor), the fourth fundamental component.

However this theory was not much practiced until 2008 when Williams made first physical memristor device at HP lab [5]. Since then it has come to the attention of many researchers. Main problem currently faced by researchers is availability of physical memristor, as it is yet to be produced commercially. That problem is greatly restricting the understanding different characteristics and possible applications. For that work on memristor mainly it is dependent on simulation or emulator of the component. Making a realistic simulation of the component itself has become an important issue. So far all the simulation of the same has been done either on active device based emulator or SPICE(Simulation Program with Integrated Circuit Emphasis). However use of SPICE simulator mainly confined among design engineer which is restricting the path for majority of the researcher. Again currently available

SPICE tools do not allow changing of device parameters while simulation is running which further restricts the understanding of the device model's applicability. Although in memristor emulators, input value can be changed in real time but main problem with them is complex physical circuitry has to be developed. To try different mathematical models, physical circuits have to be changed. All this problems regarding simulation with hardware emulator and SPICE simulator can be drastically reduced via virtual instrumentation platform such as LabVIEW, which is not much ventured yet. In LabVIEW, mathematical model of the memristor can be implemented very easily by its graphical coding technique. As the name suggests, it uses virtual instruments to design any model. So if new mathematical model has to be implemented, it can be done without any physical hardware replacement. Moreover, In LabVIEW, input signal can be varied while simulation is running which greatly facilitates the understanding of the dynamic behaviour of memristor in real time. That means it eliminates the restriction of SPICE tools to visualise output change and the requirements of complex physical circuitry of hardware emulators. Another advantage of virtual instrumentation system based simulator is that input signal can be taken from physical function generators or from virtual one and output can also be seen in virtual as well as physical oscilloscope, giving further freedom to choose signal source and output type. Here ideal HP memristor model has been demonstrated with physical signal generator and displayed the output in physical oscilloscope to show complete arrangement. However, it can be easily modified for any other complex models without any additional hardware requirement. Also virtual signal source and display can be taken very easily, eliminating the requirement of any hardware circuitry.

To do so, this paper is arranged in following way. In the section II, a general overview and types of memristor with its historical background is presented. In section III, the HP memristor mathematical model and its circuit structure is introduced. In section IV some currently available memristor simulator and emulator architectures and models are discussed. In section V basics of LabVIEW based simulator is discussed. Implementation and experimental demonstration of the implemented memristor simulator is shown in section VI and VII respectively. Finally, in section VIII, whole topic is concluded with some discussions.

II. BACKGROUND OF MEMRISTOR

According to Chua, experimental definition of a memristor can be said as any 2-terminal device exhibiting a pinched hysteresis loop which always passes through the origin in the voltage-current plane when driven by any periodic input current source, or voltage source, with zero DC components is called a memristor[6]. If the input is a current source, it is called a current-controlled memristor and if it is a voltage source, it is called a voltage-controlled one. As both are dual

to each other, once any one of them is properly defined, another one can be easily derived from that. Apart from different sources, memristor can also be classified according to the complexity of the mathematical model to derive it.

Figure 2 shows the vane diagram of different types of memristor according to their complexity where inner most circles with green colour represents simplest or ideal memristor model. Magenta and blue colour areas represent ideal generic and generic memristor model families respectively. Outer most area represents most generalised or extended generic models. For simplicity, only voltage-controlled memristor is discussed in this section (as HP memristor model is a current controlled one, and it is discussed in the next section).

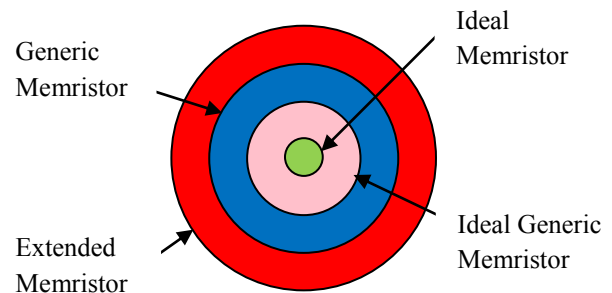


Fig. 2. Vane diagram of memristor family according to their varying complexity in mathematical model. Green circle represents the ideal memristor models which are simplest and original postulated memristor model where state variable is a direct function of charge (or current) as shown in Table 1. Magenta circle represents ideal generic version of memristor model where state variable is a piecewise differentiable 1:1 function of charge (flux). More generic version of memristor families are represented by blue circle where state variable itself is a function of input current (voltage) and complete generalised or practical memristor models are represented by the red circle.

In ideal voltage-controlled memristor, memductance which is reciprocal of memristance in case of current-controlled one is a function of flux (φ). State space representation of an ideal voltage-controlled memristor can be written as

$$i = G(\varphi) \cdot v \quad (1)$$

$$\frac{d\varphi}{dt} = v \quad (2)$$

where $G(\varphi)$ is memductance of the system.

Now (3) can be derived from (1) and (2),

$$\varphi(t) = \int v(t)dt + \varphi(0) \quad (3)$$

Once the voltage source function $v=v(t)$ and initial flux $\varphi(0)$ is given, flux wave form $\varphi(t)$ can be calculated from (3), which when substituted into memductance $G(\varphi)$, gives the time varying conductance $G(\varphi(t))$ and corresponding current waveform $i(t)$ from state dependent ohms law as described in (1). As $G(\varphi(t))$ is dependent on the initial condition or "history" of flux, it is said that this time varying conductance "memorizes" hence the name memory resistor or memristor was given.

However a memductance not necessarily has to be direct function of flux φ in fact in practical cases, memductance is not a function of flux. It can be generalised by any other piece-wise differentiable 1:1 function of the said parameter [6] and this family of memristor is called ideal generic memristor. Mathematically, voltage-controlled ideal generic memristor can be expressed as:

$$G(x).v \quad i = \quad (4)$$

$$\frac{dx}{dt} = \hat{g}(x).v \quad (5)$$

In generic cases, state variable can be a function of input variable itself and in more generic cases it memristance itself can be a function of input variable (voltage in our case). These types of memristor are called generic and extend memristor respectively. Table 1 summarises mathematical expressions of all four type of voltage-controlled as well as current-controlled memristor.

Table 1: Memristor family

Types of Memristor	Voltage controlled	Current controlled
Ideal Memristor	$v = R(q).i$ $\frac{dq}{dt} = i$	$i = G(\varphi).v$ $\frac{d\varphi}{dt} = v$
Ideal Generic Memristor	$v = R(x).i$ $\frac{dx}{dt} = \hat{f}(x).i$	$i = G(x).v$ $\frac{dx}{dt} = \hat{g}(x).v$
Generic Memristor	$v = R(x).i$ $\frac{dx}{dt} = f(x, i)$	$i = G(x).v$ $\frac{dx}{dt} = g(x, v)$
Extended Memristor	$v = R(x, i).i$ $R(x, 0) \neq \infty$ $\frac{dx}{dt} = f(x, i)$	$i = G(x, v).v$ $G(x, 0) \neq \infty$ $\frac{dx}{dt} = g(x, v)$

III. HP MEMRISTOR

Although memristor have been existing for years, they stayed unnoticed rather unexplained because this phenomenon is seen in very small scale [5]. At first physically realisable memristor and its mathematical model was developed in HP Lab it became famous in the name HP memristor. In it, a thin undoped highly resistive TiO₂ semiconductor layer and a doped highly conductive oxygen deprived TiO_{2-x} layer with initial thickness w is sandwiched between two metal contacts, as shown in Figure 3(a).

In the doping process, the negatively charged oxygen atoms are removed from its substitution site in TiO, creating a positively charged oxygen vacancy [7]. Resistances of these undoped and doped regions are considered as R_{OFF} and R_{ON} respectively as shown in Figure 3(b).

The application of an external bias $v(t)$ across the device moves the boundary between the two regions by causing the charged dopants to drift [5]. So total resistance of the device can be assumed as two variable resistors connected in series as depicted in Figure 3(c), where the resistances are given for the full length D of the device. Symbol of a memristor is also depicted in Figure 3(d). Now for the simplicity it is considered that ohmic electronic conduction and linear ionic

drift are occurring in a uniform field with average ion mobility μ_V . For a simplified case of ohmic conduction, the state-dependent current-voltage ($i-v$) relationship can be written as:

$$v(t) = \left(R_{ON} \frac{\omega(t)}{D} + R_{OFF} \left(1 - \frac{\omega(t)}{D} \right) \right) i(t) \quad (6)$$

$$\frac{d\omega(t)}{dt} = \mu_v \frac{R_{ON}}{D} i(t) \quad (7)$$

Integration of (7) yields the following formula for $\omega(t)$

$$\begin{aligned} \omega(t) &= \omega_0 + \mu_v \frac{R_{ON}}{D} \int_0^t i(t) \\ &= \omega_0 + \frac{R_{ON}}{D} q(t) \end{aligned} \quad (8)$$

By inserting (8) into (6) we obtain the memristance of this system,

$$\begin{aligned} M(t) &= R_{OFF} \left\{ \left(1 + \frac{\omega_0}{D} \left(\frac{R_{ON}}{R_{OFF}} - 1 \right) \right) \right. \\ &\quad \left. - \frac{\omega_0 R_{ON}}{D^2} \left(1 - \frac{R_{ON}}{R_{OFF}} \right) q(t) \right\} \end{aligned} \quad (9)$$

which for $R_{ON}=R_{OFF}$ simplifies to:

$$M(t) = R_{OFF} \left(1 - \frac{\mu_v R_{ON}}{D^2} \right) q(t) \quad (10)$$

The memristor behaves symmetrically when the system is within the bounded range of $M \in (R_{ON}, R_{OFF})$ and functions as a linear resistor till either one of its boundaries is reached. As long as the input polarity is not reversed it holds the resistance value [5,8,9] The charge q -dependent term on the right-hand side of this equation is the crucial contribution to the memristance, and it becomes larger in absolute value for higher dopant motilities μ_V and smaller semiconductor film thicknesses D . For any material, this term is 1,000,000 times larger in absolute value at the nanometre scale than it is at the micrometre scale, because of the factor of $1/D^2$, and the memristance is correspondingly more significant. Thus, memristance becomes more important for understanding the electronic characteristics of any device as the critical dimensions shrink to the nanometre scale. The coupled equations of motion for the charged dopants and the electrons in this system take the normal form for a current-controlled (or charge-controlled) memristor ((1) and (2)). It should be noted that HP memristor model is merely a ideal generic memristor as described in previous section. More generalised model of memristor is also came out later in different literature [10][11][12][13][14][15][16]. In next section, some of them are discussed.

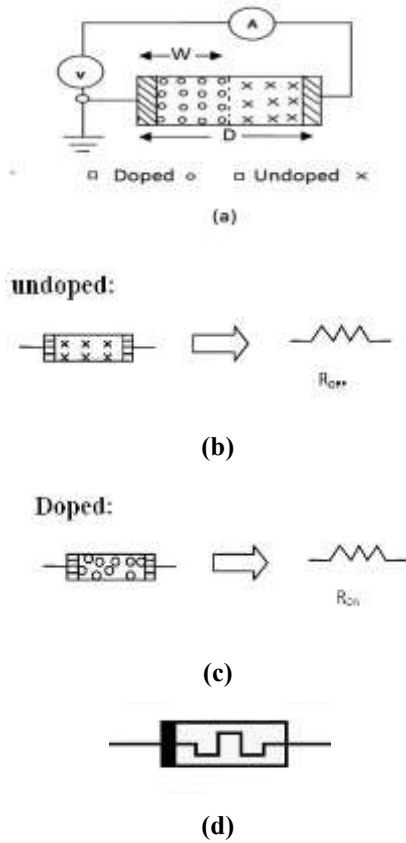


Fig. 3. The coupled variable-resistor model for a memristor. (a) Diagram with a simplified equivalent circuit V, voltmeter; A, ammeter (b) Doped region provides very low resistance whereas it is very high for undoped region. Resistances of doped and undoped regions are considered as R_{ON} and R_{OFF} respectively. (c) Total resistance for full length D of memristor is considered as serial combination of two resistors with variable length. (d) Symbol of a memristor.

IV. DEVELOPMENT OF MEMRISTOR MODELS

First generation or original HP memristor model described in [5] is popular for its simplicity but it suffers from one serious drawback. It does not take into account the boundary effects. Practically, the boundary between the doped and undoped regions, moves with speed vD in the bulk of the memristor, but this speed is strongly suppressed when it approaches either edge, $w \sim 0$ or $w \sim D$. This problem is eliminated by introducing “window function” in [10] where boundary condition is considered in state variable function and it is expressed as

$$\frac{d\omega}{dt} = \eta \frac{\mu_{DRON}}{D} i(t) F\left(\frac{\omega}{D}\right) \quad (11)$$

Where the window function $F(x)$ (x =normalised width value) satisfies $F(0) = F(1) = 0$ to ensure no drift at the boundaries and it's parameterised by a positive integer p ,

$$F_p(x) = 1 - (2x - 1)^{2p} \quad (12)$$

An alternating window function is proposed in [11] with signum function as:

$$F(x) = 1 - (x - \text{sgn}(-i))^{2p} \quad (13)$$

Although these models are simple to implement, they are not suitable for modelling of real devices as their static V-I characteristics curve refers memristor with “frozen” state variable [17]. To address this problem, non linear generic memristor models are proposed in [12] using *sinh* function for static characteristics and generalised window approach for state equation. In [12], it is shown that, in real devices (dw/dt) is determined by the drift of charged mobile ions such as oxygen vacancies. It has also been shown that at relatively high fields this drift velocity exponentially depends on the electric field

$$\frac{d\omega}{dt} \propto \sinh\left(\frac{v/E_0}{d-\omega}\right) \quad (14)$$

It also proposed that for analog memristor devices, the internal state variable w is better described as an area index rather than length index. And modified the memristor equations as

$$I = (1 - \omega)\alpha[1 - \exp(-\beta v)] + \omega\gamma \sinh(\delta v) \quad (15)$$

$$\frac{d\omega}{dt} = \lambda[\exp(\eta_1 v) - \exp(-\eta_2 v)] \quad (16)$$

where α , β , γ , δ , η_1 , and η_2 are all positive-valued parameters determined by material properties. Some further modification is done in [13] based on same analogy. However, study in [18] showed discrepancies in simulation results of these models and experimental data.

The Pickett model [14], [15], developed specifically for the TiO₂ memristor, is based on a combination of physical model of a tunnelling barrier and an empiric state equation and proposed the state variable as:

$$\omega = f_{OFF} \sinh\left(\frac{i}{i_{OFF}}\right) \times \exp\left[-\exp\left(\frac{\omega - \alpha_{OFF}}{\omega_c} - \frac{|i|}{b}\right) - \frac{\omega}{\omega_c}\right] \quad (17)$$

$$\omega = f_{ON} \sinh\left(\frac{i}{i_{ON}}\right) \times \exp\left[-\exp\left(\frac{\omega - \alpha_{ON}}{\omega_c} - \frac{|i|}{b}\right) - \frac{\omega}{\omega_c}\right] \quad (18)$$

While the model fits experimental data very well, it has been found hard to simulate [18]. This is because the static IV characteristic of the Pickett model is a multi valued function due to an inappropriate use of the Simmons model [16]. In [17] simplified pickett model is proposed which is further modified in [19]. Although some the models described so far are realised in hardware emulator [20], due to complexity involved in physical circuit design, software simulation platform SPICE is most widely used for design and validation of all the models. However, [19] showed its limitations for handling very large as well as very small parameter values. More over as discussed earlier, unlike hardware emulators, it cannot show output change with real-time input variation. To eliminate the drawbacks of both the

said platforms, and combine their advantages, National Instruments NI LabVIEW, a virtual instrumentation platform is utilised in this paper which no body have used so far. Considering this fact, in the next section concept of virtual instrumentation along with basics of LabVIEW is discussed.

V. VIRTUAL INSTRUMENTATION AND LabVIEW

In technical field, instruments are mainly used for measurement, calibration, record and display of physical parameters. It can be easily realised that with physical instruments a complete set up requires considerable amount of space and a significant amount of cost would be involved for individual instrument. More over any change in configuration of process parameters will demand different instruments and subsequent delay in reconfiguration. All the above said problems can be solved by virtual instrumentation system. Virtual instrumentation is a powerful platform where any analog signal is digitised and fed to a single computer system and the digital data is processed to simulate any said activity of any physical instrument. So replacement or modification of “instrument” can be done literally in no time with any additional space or cost.

Early virtual instrument (VI) systems were based on textual programs like BASIC, C++ or PASCAL and required technical expertise in code writing [21]. However, with the advancement of graphical user interface (GUI) based operating systems and the introduction of graphical programming technique in VI, it became more versatile, easy to use tool. NI LabVIEW is one of the finest such graphical coding platforms available till date. It cannot only simulate an instrument but also allows interfering of practical input-out signals in real time with wide variety of hardware connectivity module. This gives it the flexibility of hardware emulator to vary the input parameters in real time for better understanding which a SPICE platform seriously lags. Yet, it has all the facilities of SPICE, to modify a system without the requirement of additional physical equipments. Table 2 shows comparison of some basic features, with that of SPICE.

Table 2: LabVIEW and SPICE model comparison

Features	LabVIEW	SPICE
Real time input-output change during programme running	Possible	Not possible
Component Model availability	Not available, but can be created manually if required	Available
Circuit diagram creation	Not possible with traditional symbols of component but block diagram can be shown	Possible

Connectivity with physical world	Available, through USB	Not available
----------------------------------	------------------------	---------------

VI. IMPLEMENTATION OF MEMRISTOR

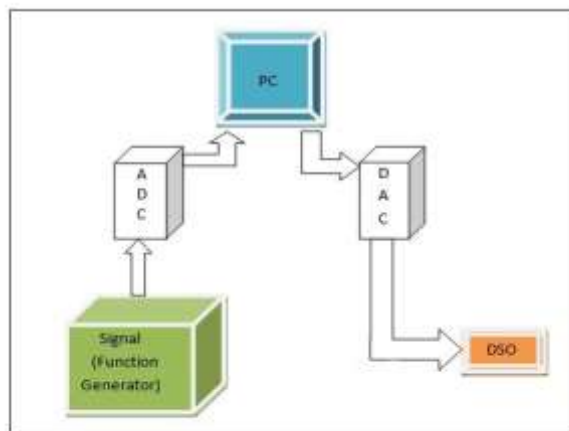


Fig 4: The block diagram of LabVIEW based memristor simulator. Analogue signal from function generator is fade to ADC unit. Digitised data is sent to the LabVIEW soft ware interface via universal serial bus (USB) data transfer system. Main mathematical model of the memristor is implemented in LabVIEW. Output of the model circuit is sent to the DAC block for equivalent analogue signal output which is sent to DSO for display.

The memristor simulator has been implemented in such a way that the input resistance is calculated as a function of the applied current or voltage to satisfy the equations of the memristor given in ((1), (2)). The working principle of the simulator is simple. Analog signal from the function generator is continuously quantised and digitised by Analog to digital converter (ADC). Equivalent digital signal is feed to the input of the simulator block. Interfacing between ADC and LabVIEW software is done through Universal Serial Bus(USB) interface. Resultant digital output goes to the digital to analog converter (DAC) which is fed to any external or internal circuitry as required. Here digital storage oscilloscope (DSO) is used in XY mode to show the basic voltage current characteristic behaviour of the simulator. Block diagram of the total system is shown in the figure 4. Although for greater applicability demonstration, physical function generator and DSO are used here, LabVIEW provides both function generator and oscilloscope virtually. Equations of the state dependent current–voltage (i–v) relationship of the ideal generic memristor (HP memristor model) which were presented in the section III have been implemented on the LabVIEW and executed with input signal from function generator.

A summary of the characteristics of the simulator and its comparison with the actual physical device is presented in Table 3.

Table 3:Characteristic of the simulator and comparison with the physical device.

Parameter	Physical device	Simulator	Description
Resistance range	Determined by device structure	$0 < R < 10E+308 \Omega$	Maximum length of a number in LabVIEW can be used as resistance value
Discretisation of R	Continuous	Maximum $10E+615$ steps	$10E+307$ steps between each pair of $10E+308$ values
Response	Determined by device structure	Programmed function	Mathematical model
Applied voltage	Less than device structure breakdown voltage	0V (input adc voltage)	24 bit Unipolar ADC (for physical input model)
Output voltage	Less than device structure breakdown voltage	5 volt	10 bit DAC (for physical output model)
Supply voltage	-----	$V_{ss}=0, V_{dd}=5V(ADC)$ $V_{ss}=0 V_{dd}=5v(DAC)$	Power supply

VII. EXPERIMENTAL SETUP AND RESULTS

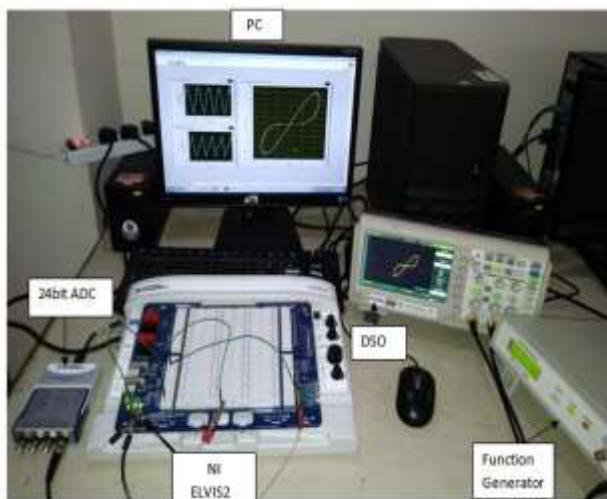


Fig. 5. Experimental setup for evaluation of memristor model in LabVIEW.

Set up is used to validate the model as shown in figure 5. Here input sinusoidal signal is fed to a 24 bit high resolution ADC module of National Instruments via a 50 ohm BNC connector. Quantised and digitised signal data from this module is feed to LaVIEW (in computer system) using USB(Universal Serial Port) connector with a baud rate of 115200.Data coming from the designated USB port is collected by Data acquisition module(DAQ) which is set for collecting data from analogue port0 in terms of voltage. Maximum input voltage range, given to DAQ was +-10 volt and set to constant sampling mode with sampling rate of

1kHz.

InLabVIEW, output of the DAQ module was passed through an integrator block followed by some arithmetic blocks to create a complete equation of ideal memristor as described in ((1), (2)).Output of arithmetic modules along with original input is fed to output module of LabVIEW which was set for interfacing with two 12 bit DAC outputs, present in NI ELVIS development board which is connected to computer system via USB port.Output module of LabVIEW was programmed for max output range of +-10volts with sampling frequency of 1kHz in continuous sampling mode. Output of DAC from ELVIS boards is sent to Digital Storage Oscilloscope (DSO)with maximum input frequency of 50MHz via two 50 ohm BNC connectors. To get the characteristic curve (pinched hysteresis loop) in DSO,it was set to XY mode which plots one input channel data with respect to another instead of plotting channel data separately with respect to time.

Initially a sinusoidal input signal with maximum amplitude of $10\mu A$ and frequency 10 Hz was fed to the system. From i-v plot the pronounced pinched hysteresis loop was observed from thatwhich expectedly shrinks with an increase in frequency which is again observed for frequencies of 20 Hz, 30 Hz, 40

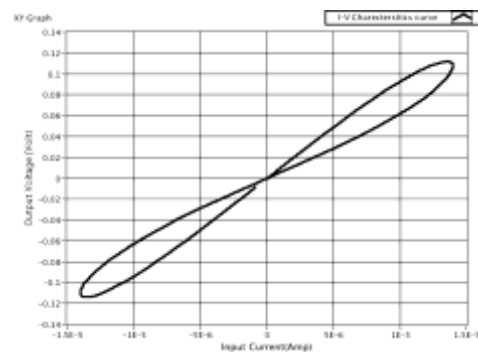
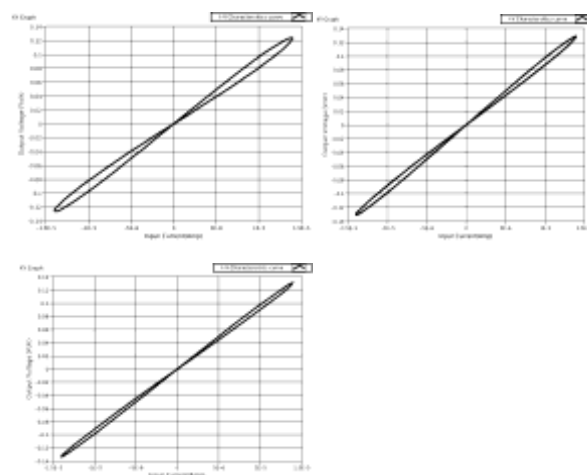


Fig. 6. Output curve for 10Hz

Hz and 50 Hz respectively. Figure 6 to 10 shows the shrinkage of curve with the increment in frequency thus



validating the basic fingerprint of a memristor. Figure 11

shows the charge and flux relation of the implemented system

Fig.7.Output for 20Hz
Fig. 9. Output for 40Hz

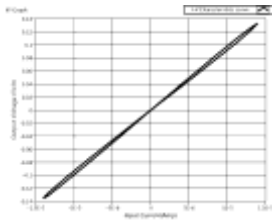


Fig. 8. Output for 30Hz
Fig.10 Output for 50Hz

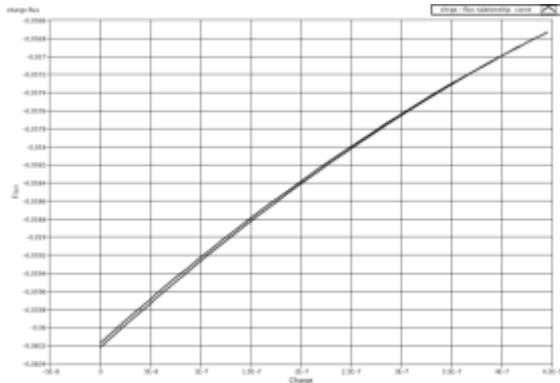


Fig.11 Charge Vs. Flux curve

Regarding some discussions on some features or limitations of the system is that DAC used by the ELVIS 2 board is of 12 bit which refers maximum difference between two signals it can show is 4096 times of each other, but for memristor configuration with $R_{OFF}=10k$, the difference between input and output is 10,000 times to each other which means a 14 bit (maximum difference 16,384) DAC is required if both input and output signals are to be collected from DAC. Again, output from DAC below 10 mV becomes too much noisy which needs further filtering before giving it to the oscilloscope input. However it would not be a problem if input signal is directly taken from function generator itself. Again if virtual plotter is used there would be no problem at all. So while using it for physical circuit and output signal is taken from DAC module, input should be taken from function generator directly if the resolution of DAC module is less than 14 bit.

VIII. CONCLUSION

From the above discussions it can be concluded that, as physical memristor is yet to be commercialised, it is very important to create a reliable simulation model and easy to use platform for analysis and its application possibility for. For that, choosing a convenient, easy to use platform is of equal importance. From the above discussion it can be said that NI LabVIEW provides all the advantages of both emulator and simulator with greatly increased parameter ranges and allows to interface with physical devices making it far more versatile than traditional SPICE based simulators.

So along with the available hardware emulators and SPICE based software simulators, it can be a good alternative development platform.

REFERENCES

- [1] Liang, W., Shores, M. P., Bockrath, M., Long, J. R., & Park, H. (2002). Kondo resonance in a single-molecule transistor. *Nature*, 417(6890), 725-729.
- [2] Cole, K. S. (1972). *Membranes, ions and impulses: a chapter of classical biophysics* (Vol. 5). Univ of California Press.
- [3] Mauro, A. (1961). Anomalous impedance, a phenomenological property of time-variant resistance: An analytic review. *Biophysical Journal*, 1(4), 353-372.
- [4] Chua, L. (1971). Memristor-the missing circuit element. *IEEE Transactions on circuit theory*, 18(5), 507-519.
- [5] Strukov, D. B., Snider, G. S., Stewart, D. R., & Williams, R. S. (2008). The missing memristor found. *nature*, 453(7191), 80-83.
- [6] Leon, C. H. U. A. (2015). Everything you wish to know about memristors but are afraid to ask. *Radioengineering*, 24(2), 319.
- [7] Y. Ho, G.M. Huang, P. Li, Dynamical properties and design analysis for nonvolatile memristor memories, *IEEE Trans. Circuits Syst. I: Regul. Pap.* 58 (4) (2011) 724-736.
- [8] M.P. Sah, C. Yang, H. Kim, L. Chua, A voltage mode memristor bridge synaptic circuit with memristor emulators, *Sensors* 12 (3) (2012) 3587-3604.
- [9] Z. Biolek, D. Biolek, V. Biolkova, Spice model of memristor with nonlinear dopant drift, *Radioengineering* 18 (2) (2009) 210-214.
- [10] Joglekar, Y. N., & Wolf, S. J. (2009). The elusive memristor: properties of basic electrical circuits. *European Journal of Physics*, 30(4), 661.
- [11] Biolek, Z., Biolek, D., & Biolkova, V. (2009). SPICE Model of Memristor with Nonlinear Dopant Drift. *Radioengineering*, 18(2).
- [12] Chang, T., Jo, S. H., Kim, K. H., Sheridan, P., Gaba, S., & Lu, W. (2011). Synaptic behaviors and modeling of a metal oxide memristive device. *Applied Physics A: Materials Science & Processing*, 102(4), 857-863.
- [13] Yakopcic, C., Taha, T. M., Subramanyam, G., & Pino, R. E. (2013). Generalized memristive device SPICE model and its application in circuit design. *IEEE Transactions on Computer-Aided Design of Integrated Circuits and Systems*, 32(8), 1201-1214.
- [14] Pickett, M. D., Strukov, D. B., Borghetti, J. L., Yang, J. J., Snider, G. S., Stewart, D. R., & Williams, R. S. (2009). Switching dynamics in titanium dioxide memristive devices. *Journal of Applied Physics*, 106(7), 074508.
- [15] Abdalla, H., & Pickett, M. D. (2011, May). SPICE modeling of memristors. In *Circuits and Systems (ISCAS), 2011 IEEE International Symposium on* (pp. 1832-1835). IEEE.
- [16] Kolka, Z., Biolek, D., & Biolkova, V. (2015). Improved model of TiO₂ memristor. *Radioengineering*, 24(2), 378-383.
- [17] Kolka, Z., Biolkova, V., & Biolek, D. (2015, November). Simplified SPICE model of TiO₂ memristor. In *Memristive Systems (MEMRISYS) 2015 International Conference on* (pp. 1-2). IEEE.
- [18] Linn, E., Siemon, A., Waser, R., & Menzel, S. (2014). Applicability of well-established memristive models for simulations of resistive switching devices. *IEEE Transactions on Circuits and Systems I: Regular Papers*, 61(8), 2402-2410.
- [19] Biolek, D., Biolkova, V., & Kolka, Z. (2017, June). Modified MIM model of titanium dioxide memristor for reliable simulations in SPICE. In *Synthesis, Modeling, Analysis and Simulation Methods and Applications to Circuit Design (SMACD), 2017 14th International Conference on* (pp. 1-4). IEEE.
- [20] Olumodeji, O. A., & Gottardi, M. (2017). Arduino-controlled HP memristor emulator for memristor circuit applications. *Integration, the VLSI Journal*.
- [21] Evolution of virtual instrumentation: <https://www.scribd.com/document/38417513/Evolution-of-Virtual-Instrumentation>/Accessed 9th November, 2017